Chapter 8
DNA Knots

Cristian Micheletti

Abstract Knotting is statistically inevitable in long polymer chains, especially under spatial confinement, and tightly packed genomic DNA filaments are no exception. Over several decades, ever more powerful experimental techniques have demonstrated the occurrence of knots and other forms of entanglements in DNA extracted from viruses, bacteria, and eukaryotes. The data have in turn prompted a broad range of theoretical and computational studies of the abundance and complexity of DNA knots, and especially: (i) how it depends on the length and degree of confinement of the filaments (ii) whether it can be used to infer the multiscale spatial organization of genomic DNA, and (iii) its impact on biological processes in vivo. Here, we present an overview and a personal perspective of such theoretical and experimental efforts, from the equilibrium knotting of DNA in bulk to the one observed in various organisms, and concluding with a comparison with RNAs and their entanglement properties.

8.1 Introduction

We are all familiar with the inconveniences posed by knots and other entanglements that arise in long cables that have been carelessly stored away.

We also know how challenging it is to arrange a ribbon or a rope in a desired knotted shape for decorative or functional purposes, a task for which we usually necessitate step-by-step guidance from a good knot book [1].

Our intricate relationship with macroscopic knots occurs between these two extremes: preventing or fighting against the statistical incidence of knots and creating or designing knots for specific functions.

A similar balancing act is continuously taking place at a molecular level in all organisms, from viruses to bacterial and eukaryotic cells, where active (enzyme

C. Micheletti (✉)
SISSA, Via Bonomea 265, 34136 Trieste, Italy
e-mail: michelet@sissa.it

© The Author(s), under exclusive license to Springer Nature Singapore Pte Ltd. 2022

Y. Tezuka and T. Deguchi (eds.), *Topological Polymer Chemistry*,
https://doi.org/10.1007/978-981-16-6807-4_8

mediated) and passive (physics mediated) mechanisms control the entanglement of different types of biopolymers in vivo.

Nucleic acid filaments offer, perhaps, the best illustration of biomolecular entanglement. In all organisms, genomic DNA filaments are confined in regions much smaller than their contour length, a situation that already makes them prone to spontaneous entanglement. In addition to this, the incessant DNA processing during transcription, replication, and recombination accumulates DNA entanglements that can be lethal for the cell and, thus, must be efficiently removed by specialized enzymes [2–4].

At the other extreme we have RNAs, where no physical knots have been discovered yet [5, 6]. Unlike double-stranded DNA, which can be often modelled as a fluctuating filament, naturally occurring RNAs have definite folds that, though physically unknotted, can still be intricate. In this case, too, RNA entanglement appears to be instrumental for specific biological functions, such as inducing ribosomal frameshifting [7–10] or stalling the action of degrading enzymes [11–17].

Our understanding of these manifestations of physical entanglement in nucleic acids has increased immensely in recent years, thanks to parallel theoretical and experimental advancements [18–21]. Thanks to these interdisciplinary and still ongoing efforts we have gained much insight into the general mechanisms that control knot abundance, size, and complexity in these biomolecules, and clarified the functional implications, too.

Here, we present an overview and personal perspective of such theoretical and experimental findings starting from DNA knotting in bulk, then moving to the knotting of genomic DNA in various organisms, and finally discussing on RNA entanglement.

8.2 Spontaneous Knotting of DNA in Solution

8.2.1 Experimental Results

A natural starting point is the entanglement of DNA filaments that fluctuate freely in solution. A landmark study was carried out by Rybenkov et al. who considered 10kb-long DNA filaments from P4 viral particles [22]. The DNA of these bacteriophages is double-stranded except for the two termini, which are single-stranded and have complementary sequences. Thus, when the two termini come in contact, they can anneal and turn the DNA from linear to circular.

Such stochastic cyclization events make it possible to turn the transient physical entanglement of fluctuating linear DNA filaments into proper knotted states of the circularized DNA [23].

The abundance and complexity of knots in cyclized DNA were then established using gel electrophoresis. The gel matrix constitutes an array of obstacles that the DNA rings have to negotiate when drawn through the gel by an electric field. The

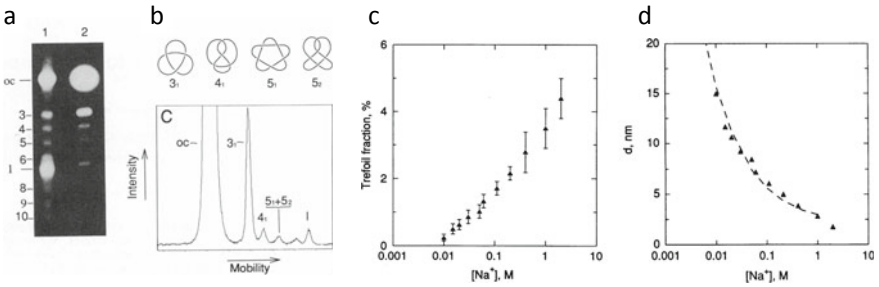

Fig. 8.1 **a**, **b** Gel-electrophoretic separation of DNA knots. **c** Fraction of cyclized DNA rings with trefoil knot topology as a function of the concentration of monovalent counterions in solution. **d** Effective DNA diameter, theoretical-inferred from the observed knotting probability, as a function of counterion concentration. Reproduced with permission from Ref. [22]. Copyright (1993) National Academy of Sciences, U.S.A

DNA rings' capability to slide through or past the obstacles depends on their topological state [24–28]. Accordingly, DNA rings with different knot types acquire different electrophoretic velocities and form distinct gel bands. The bands' intensities can then be used to quantify the relative abundance of the various types of knots; see Fig. 8.1a, b. Similar electrophoretic principles are conventionally used to separate DNA molecules by length or degree of supercoiling, as these properties too are coupled to gel mobility [29]. For this reason, electrophoretic topological profiling requires DNA rings to be of the same length and free of torsional stress, which is the case for the doubly nicked P4 DNA rings.

Using this technique, Rybenkov et al. were able to profile the type and abundance of DNA knots at different monovalent salt concentrations [22]. At these chain lengths, the most abundant type of non-trivial knots is the trefoil one, whose incidence as a function of the solution ionic strength is shown in Fig. 8.1c.

Two notable features emerge from the experimental results. First, the knot spectrum is dominated by trefoil knots, the simplest knot type, with only traces of more complex topologies. Second, the unknotting probability, which is the probability of unknotted DNA rings, decreases rapidly with the solution's ionic strength.

8.2.2 Theoretical Modelling and Interpretation

The results can be qualitatively rationalized in terms of the electrostatic screening operated by dissolved counterions.

Salt concentration controls both the effective DNA charge density via counterion condensation and the Debye screening length. To a first approximation, the DNA screened self-repulsion can be treated as an effective increase in DNA diameter. By increasing the solution's ionic strength, the Debye screening length and hence the

effective DNA thickness decrease. Because the DNA contour length is unchanged, a diameter reduction induces an enhanced knotting probability.

These qualitative considerations were turned into quantitative ones using stochastic simulations on a coarse-grained DNA model [22]. Circularized P4 DNA rings were modelled as a semi-flexible ring of cylinders of length l and diameter Δ. The cylinders' length was set to be $l = 10$ nm, a fraction of the nominal DNA persistence length $l_p \sim 50$ nm. The latter was accounted for by a bending energy term for consecutive (hinged) cylinders. At the same time, excluded volume interactions were enforced by preventing non-consecutive cylinders from overlapping.

A Monte Carlo scheme was next employed to sample the equilibrium ensemble of the model rings. The Monte Carlo evolution involved the use of crankshaft moves to rotate a portion of the rings. The moves do not disconnect the chain but can alter the ring topology. The two conformations before and after the move must be self-avoiding to be part of the Monte Carlo trajectory. However, the continuous deformation bridging the two states can still involve "unphysical crossings" of the cylinders. The Monte Carlo evolution can, thus, introduce or remove knots, which can be detected by computing topological invariants.

The ensemble generated by such Monte Carlo scheme is often referred to as "topologically unrestricted ensemble", and sampled conformations are expectedly equivalent to those obtained by circularisation in equilibrium.

The Monte Carlo sampling of this ensemble was used to reproduce and interpret the experimental knotting data from P4 cyclization [22]. Specifically, the topological spectrum was computed by keeping fixed the contour and persistence length of the model DNA rings and varying the cylinders' diameter. Finally, for each ionic strength condition, it was determined which diameter gave the best match between the computed and experimental knot spectra.

This strategy allowed for inferring the effective thickness of DNA from experimental data on equilibrium knotting probabilities; see Fig. 8.1d. The recovered functional dependence of DNA diameter on salt concentration was in good agreement with polyelectrolytes theory. The results confirm a posteriori the theoretical framework's viability to correctly reproduce the physical properties of fluctuating DNA filaments, knotting included.

To summarize, the seminal study of Rybenkov et al. allowed for establishing the following results and concepts.

First, fluctuating filaments of dsDNA even as short as 10kb can present detectable levels of spontaneous knotting. Second, these knots were detected after being trapped by DNA circularization, but clearly, they pre-existed as "physical knots", or knots in open chains. Third, the experimental DNA knotting probability and topological spectrum are well accounted for by coarse-grained models, making them an essential ally to experiments. Modelling and simulations can provide quantitative physical interpretations of experimental data. When used predictively, they can help design or precondition experimental setups and discover emergent phenomena verifiable in the lab.

The coarse-grained model used in Ref. [22] has provided the bases for many later studies. Its physical appeal rests in the fact that it is informed by three physical length scales only. These are the DNA thickness, persistence length, and contour

length. In fact, we note the choice of the cylinders' length is immaterial as long as it is sufficiently smaller than the persistence length [22]. Thus, it is presently more common to use chains of beads in place of chains of cylinders.

The interplay of all these lengthscales and their effect on knotting has been systematically addressed in a large number of studies where contour length [30–34], chain diameter [35–37], and persistence length [38–41] were systematically varied. Though we still lack a general theory of polymer entanglement, these length scales are recognized as central to knotting and are used in scaling approaches for recapitulating knotting properties across various contexts and models [42, 43].

8.3 Native Knotting of Genomic DNA

8.3.1 Viral DNA

The sizeable knotting found in the 10kb-long P4 genome in solution prompts the question of how much more entangled the same viral DNA filaments can become inside the P4 capsid, where it is stored at high packing densities.

This point was quantitatively addressed by Roca et al. in a series of experiments on P4 mutants [44–46]. Unlike the wild-type P4, where one of the DNA ends is secured to the virus tail, the genome of these mutants is fully loaded inside the capsid. As in the bulk experiments of Rybenkov et al., the annealing of the two ends can, thus, trap any entanglement of the packaged DNA as proper knotted states of the cyclized genome [44]. The circularized DNA extracted from an ensemble of viral particles can then be topologically profiled using gel electrophoresis.

The resulting topological spectrum highlighted three main features. First, the extracted DNA was knotted in more than 95% of the cases [44]. Second, the spectrum contained knots with large crossing numbers, a standard measure of knot complexity [44]. Finally, torus knots were significantly over-represented in the topological spectrum [45]; see Fig. 8.2.

These features provide important clues about the organization of DNA inside viral particles. The varied topological spectrum, covering different knot types, directly proves that DNA packing inside viral capsids is structurally heterogeneous. Instead, the over-representation of torus knots in the spectrum indicates an overall spool-like arrangement of the packed DNA.

Above all, the pervasive amount of knotting was particularly surprising and also perplexing considering the expected obstacle it could pose to viral genome delivery. In fact, it posed a conundrum: how is it possible that the knotted DNA can be ejected through the exit channel that is too narrow to allow for the simultaneous occupation by multiple DNA strands [47, 48]?

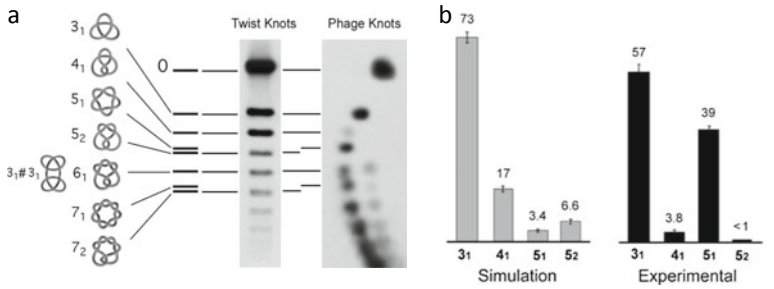

Fig. 8.2 **a** Gel-electrophoretic separation of different knot types established by 10kb-long DNA inside P4 viral capsid. **b** Comparison of the relative (percentage) incidence of the four simplest knot types in experiments and in a general model of confined polymer. The DNA bias towards forming torus knots inside capsids is apparent from experimental data. Reproduced with permission from Ref. [45]. Copyright (2005) National Academy of Sciences, U.S.A

8.3.2 Theoretical Modelling and Interpretation

Coarse-grained models have proved very valuable to gain insight in all the above aspects [48, 49] and helped unveil the surprising physical mechanisms underpinning them.

From a qualitative point of view, the high overall incidence of viral DNA knotting is well accounted for by the high level of confinement. Various studies have addressed the knotting of equilibrated rings in three-dimensional confinement with molecular dynamics and the Monte Carlo simulations.

The first such study was arguably carried out by Michels and Wiegel, who profiled the knot spectrum of infinitely thin and fully flexible equilateral rings inside spherical cavities and observed that the knotting probability increased rapidly with the packing fraction [51]. More precisely, the incidence of unknots, that is, of rings with the trivial

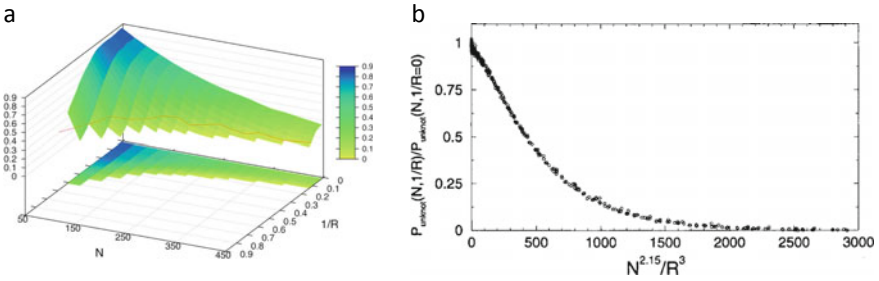

Fig. 8.3 **a** Manifold of the unknotting probability inside spheres of radius R. Data are for rings of $50 \leq N \leq 450$ edges. **b** The same data points collapse on a single curve when plotted as a function of $N^2.15/R^3$. Reproduced with permission from Ref. [50]

(unknotted) circular topology, was not controlled by the mere packing density, N/R^3, but by a different scaling parameter, N^α/R^3 with $\alpha \sim 2.2$ [50, 52]; see Fig. 8.3.

These results, thus, help rationalize the overall high abundance of knots found inside viral capsids, as fully flexible equilateral rings can be taken as a crude model of circularized DNA, with the bond length corresponding to the Kuhn length. Incidentally, we note that thermal fluctuations that establish canonical equilibrium are essential to introduce knotting in the confined rings. In fact, DNA packing models at zero temperature, i.e. energy-minimizing configurations, yield ordered spools that are virtually knot-free [53].

Though the overall high incidence of DNA knots is accounted for by general models of confined polymers [50, 54], the same models fail to reproduce the key features of the knot spectrum, such as the characteristic over-representation of torus knots.

This is well illustrated by the relative abundance of 5_1 and 5_2 knots, which have the same nominal complexity (5 crossings in their simplest diagrammatic representation) but one belongs to the torus knots family and the other to the twist knot family. At all levels of spatial confinement of infinitely thing rings, the population of 5_2 knots is usually twice as abundant as the 5_1 knot, see e.g. simulation data in Fig. 8.2b. The result holds more in general, as it applies to other common models of rings, such as semi-flexible rings of cylinders or semi-flexible chains of beads, and, thus, reflects the larger configurational entropy of 5_2 knots compared to 5_1 ones [49, 50, 54, 55]. However, the opposite bias is observed in viral DNA, see experimental data in Fig. 8.2b. One, thus, concludes that the strong bias towards torus knots observed experimentally is due to specific properties of DNA packing that are not captured by general polymer models.

The conundrum was clarified in the study of Ref. [49], which noted that the DNA packing density inside viral capsids is sufficiently high to cause a local cholesteric ordering of contacting DNA strands. This cholesteric ordering follows from the double-helical nature of DNA, which causes contacting strands to juxtapose at a preferred angle. The study then showed that when propensities for local cholesteric ordering are included in DNA models, the knot spectrum acquires the correct bias towards torus knots, and even a quantitative agreement with experimental data can be reached; see Fig. 8.4a.

The good match of the topological spectra from theory and experiment is an appealing result per se but has broader implications, too. It validates a posteriori the coarse-grained model and, thus, gives confidence for using it to capture the DNA structural organization under spatial confinement. Typical model DNA configurations inside spherical cavities, an approximation to viral capsids, are shown in Fig. 8.4b, where they can be contrasted with those obtained without the cholesteric interaction term. The differences in arrangement are very noticeable, with the refined model showing an enhanced ordering of the DNA in layered shells. The order, however, is not perfect as regions at large sequence separation can be stacked one upon the other (as denoted by the different colours of the juxtaposed regions), and the winding directionality is not necessarily constant.

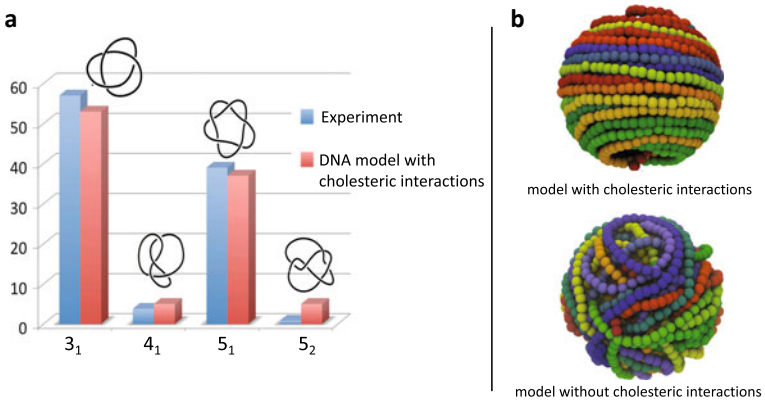

Fig. 8.4 **a** Accounting for DNA cholesteric interactions allows to reproduce the experimental topological spectrum of DNA inside capsids. **b** Including or excluding cholesteric interactions significantly affects the arrangement of the confined model DNA. Reproduced with permission from Ref. [49]

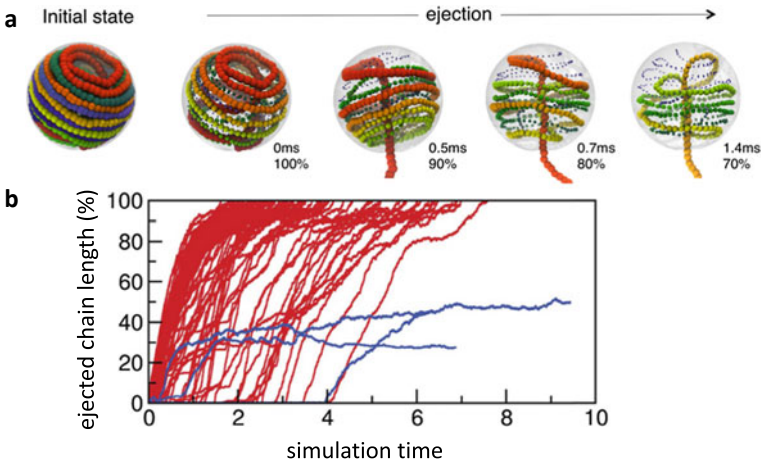

Fig. 8.5 **a** Snapshots from simulations where knotted DNA ejects from a model spherical capsids. **b** Time evolution of the ejected chain fractions over the independent realization of the process. In only a small fraction of the trajectories, the presence of the knot hinders the translocation process. Reproduced with permission from Ref. [48]

The same model was subsequently used to study the ejection process and solve the puzzle of how the viral DNA could exit from the capsid through a narrow pore despite being highly knotted [48].

Inspection of the trajectories clarified the underlying physical mechanism. The high degree of confinement causes the knot to be delocalized over most of the DNA contour. Because the knot is widely spread, the continuous rearrangements of the chain facilitate the strand passages leading to a progressive untying of the DNA as

more of it is ejected from the pore. In practice, knot complexity diminishes in parallel with the length of the chain inside the capsid; see Fig. 8.5.

This simplification would not be possible if the knot were tight, a condition that is prevented by confinement. The results, thus, highlight a dual effect of capsid confinement on DNA: it boosts the entanglement of the packaged DNA but, because it causes knot delocalization, it also facilitates the smooth ejection of knotted DNA.

8.3.2.1 Pore Translocation of Tightly Knotted Filaments

The results discussed above leave unanswered a more general issue: how is polymer translocation affected by tight physical knots? The question is relevant in the many contexts where pore translocation is used to profile the physical properties of polymers [56–61] and in applicative contexts too, such as the sequencing of single-stranded DNA [9, 62–64, 64–68, 68–73]. In the latter setups, an electric field applied along the pore axis is used to drive through the pore the DNA strand along with ions in solution. The temporal modulation of the ionic current through the pore can then be used to infer the chemical identity of the nucleotides as they pass through the pore.

The pore translocation of (unknotted) polymer chains is a classic problem in polymer physics, which is now relatively well understood [56, 58, 61, 74–76]. The translocation response is dictated by the tension propagating from inside the pore, where the driving force is applied, to the rest of the chain.

The simulations of Ref. [77] showed that the propagating tension causes the tightening of the knots in the translocating chain. The tightened knots eventually reach the pore where they are pulled even more tightly against the outer surface of the pore.

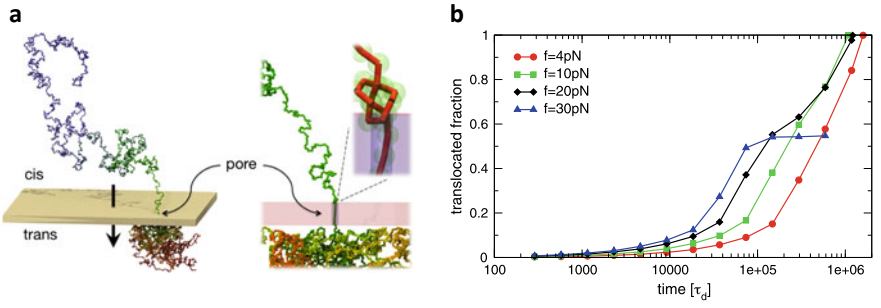

Fig. 8.6 **a** Initial stages of the driven translocation of a knotted chain through a narrow pore. The chain is modelled as a fully flexible string of beads. **b** Temporal traces of the translocated chain fraction. The presence of the tight knot at the pore entrance can stall translocation only at sufficiently large driving forces. Reproduced with permission from Ref. [77]

Our everyday experience with macroscopic ropes suggests that the translocation of a knotted rope should stall when the knot reaches the pore entrance in a tight form due to the significant friction developed in the knotted region.

However, the results of Ref. [77] demonstrated that this intuitive picture is not necessarily applicable to microscopic situations.

In fact, it was observed that tight knots do not per se prevent translocation of chains of beads, as illustrated in Fig. 8.6. In this context, unlike the macroscopic case, thermal fluctuations allow the beads in the knotted portions to overcome the barriers of the corrugated potential created by the tightly contacting portions of the knot that slide relative to each other. Thermal fluctuations, thus, allow the knot to "breathe" and overcome these microscopic realizations of friction and, thus, slide along the knotted chain contour.

Thanks to this mechanism, chains can slide and translocate through narrow pores even when they accommodate tight knots. However, applying sufficiently high driving forces eventually causes such a tight interdigitation of the beads that thermal fluctuations cannot compete with frictional effects anymore [77]. When this happens, one recovers the intuitive stalling of translocation in knotted macroscopic ropes.

Since it has been first reported, this mechanism has been found in other contexts too and, for instance, has been argued to be relevant in connection to protein degradation by the proteasome [78–83].

8.3.3 Bacterial DNA

Knots have long been known to occur in bacterial DNA too, which is organized in circular form [84, 85]. Unlike the case of viral DNA knotting, which occurs inside the capsid, the knotting of bacterial DNA is created by the action of enzymes during, e.g. transcription or replication [2, 86–88].

The entanglement that is inevitably created during these processes is continuously relieved by topoisomerase enzymes, which come in two types or classes [89]. Type I topoisomerases act by cutting only one strand of the DNA double helix and allowing it to swivel around the other strand. This mechanism does not alter the topology of DNA plasmids or circular chromosomes. It is instrumental for achieving the torsional relaxation of the chain and for controlling its degree of supercoiling, that is, the level of over or underwinding (bacterial DNA is kept at around 0.05 negative supercoiling density).

Type II topoisomerases cut both strands and, by assisting the passage of another DNA strand through the cut, can alter DNA topology [84, 90, 91]. The action of type II topoisomerases is, thus, crucial to eliminate detrimental forms of DNA entanglement [88, 92, 93]. For instance, newly replicated plasmids are catenated and must be unliked via suitable strand passages for correct subdivision into daughter cell to proceed [94, 95]. Similarly, topoisomerases must efficiently remove DNA knots, such as those created by concurrent replication and transcription activities, and whose accumulation would be detrimental and even lethal for the bacterial cell [91, 93, 96].

Many efforts have been spent to rationalize how these enzymes, which are too small to "sense" the global DNA topology, can recognize and perform the correct strand passages leading to knot simplification. Random passages would yield the "equilibrium" knotting observed in random cyclization, and topoisomerases can bring knotting much below this equilibrium level.

Several elegant and physically appealing suggestions have been made over the years to reconcile the local action of topoisomerases with the resulting global simplification of DNA topology.

These suggestions include the recognition by topoisomerases of local geometrical features that are over-represented in knotted DNA rings. These notably include so-called hooked juxtapositions of DNA strands, which corresponds to DNA strands that are contacting so tightly that they establish a clasp [97–100]. These clasps are distinctive of essential crossings in tight knots, but they occur in delocalized knots too. Numerical simulations on various models have verified that strand passages at hooked juxtapositions can indeed take the knotting probability well below the equilibrium values. Interestingly, recent modelling work by Ziraldo et al. [101] has shown that clasp condition can be relaxed and that topological simplification can be achieved by performing crossings in correspondence of juxtapositions where one strand is bent around the other. Other invoked mechanisms involve the actual localization of the knot itself, for instance by accumulated supercoiling [102–105].

The simultaneous presence of DNA knotting and supercoiling is particularly interesting as it combines geometrical and topological entanglement. How exactly the two affect DNA conformational dynamics is a particularly relevant issue for bacterial DNA, and it was recently tackled in Ref. [106] with molecular dynamics simulations of 2kb-long DNA rings with supercoiling and/or 5-crossing knots. The rings' length and topology were chosen to approximate those reported experimentally [2, 84].

Analysis of trajectories showed that when either supercoiling or knotting were individually present, DNA rings retained substantial conformational freedom. The rings could, in fact, interconvert between states with different numbers of plectonemes or localized and delocalized knot states [106], see Fig. 8.7.

However, when both knotting and supercoiling were present, the reconfiguration dynamics was dramatically slowed down. The location of the essential crossings of the knotted region and of plectonemes remained locked over timescales at least an order of magnitude longer than when either knots and supercoiling alone are present. In fact, the location of plectonemes and knot crossings persisted for the entire simulated trajectories; see Fig. 8.7.

The slowed conformational dynamics is an unexpected emergent property of knotted and supercoiled rings that can illuminate a thus far underexplored aspect of DNA topological simplification. A pre-requisite for topoisomerases to detect and remove essential crossings is that the distinctive local geometry of the latter persists long enough to be recognized.

This temporal element, which had been envisioned in Ref. [107], is still beyond the reach of current experimental probing techniques, and numerical simulations and modelling are currently our best source of insight into this fascinating subject.

8.3.4 *Eukaryotic DNA*

It is only recently that experimental breakthroughs have allowed for probing the knotting properties of eukaryotic DNA. This feat was recently accomplished by Roca's lab with a series of studies on the in vivo topological entanglement of YRp4 yeast minichromosomes [108, 109].

These circular minichromosomes are 4.4kb long, involve ∼25 nucleosomal units, and are typically maintained at a negative level of supercoiling. Using gel electrophoresis, it was established that the typical in vivo level of knotting was about 2% [108]. The result is noteworthy in several respects. First, it gave a first demonstration that even very short eukaryotic DNA is knotted in vivo. Second, the observed knotting is substantially different from the one of DNA rings of similar length that circularize in solution. Additionally, the knot spectrum is biased in favour of left-handed knots, again differently from the case of random circularisation in solution [108]. These topological differences, thus, follow from the specific spatial arrangement of eukaryotic DNA, including its torsional stress associated with wrapping around nucleosomes and the overall degree of supercoiling.

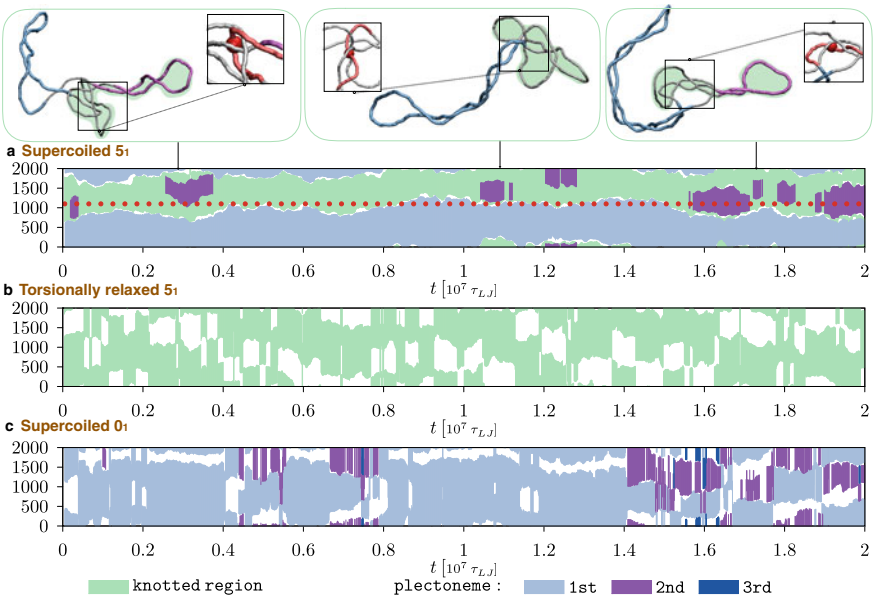

Fig. 8.7 Kymoplots showing the position of the plectonemes and/or the knotted region in a model 2kb-long DNA ring. The first kymoplot is for the supercoiled unknotted chain, the second is for a knotted but torsionally relaxed chain, and the third is for a knotted supercoiled chain. The persistence of plectonemes and knot boundaries in the latter is apparent. Reproduced with permission from Ref. [106]

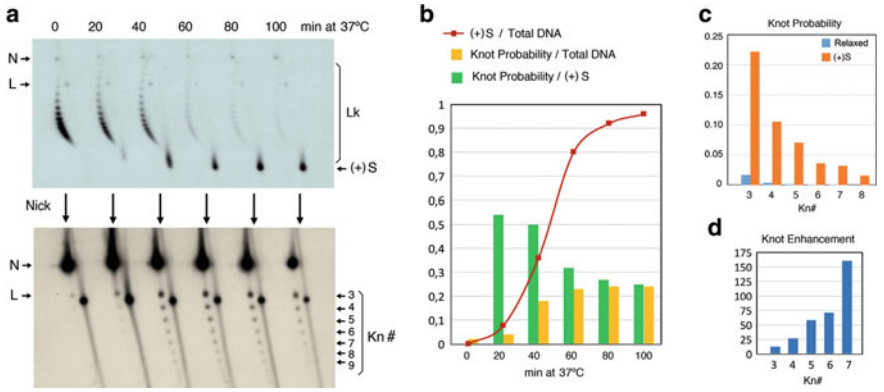

Fig. 8.8 Electrophoretic traces and measurements showing the increasing incidence of knots and positive supercoiling, (+S), accumulated during transcription of yeast minichromosome YRp4. Reproduced with permission from Ref. [109]

A subsequent study succeeded at probing the amount of knotting that is generated during transcription/replication [109]. When the two DNA strands are pulled apart, negative and positive supercoiling is generated, respectively, behind and ahead of the transcribing machinery. The ensuing torsional stress and entanglement are relaxed by the action of both type I and type II topoisomerases; the latter, we recall, can alter DNA topology.

The topological profiling at different transcription stages gave remarkable results. During transcription, knotting was boosted up to an approximately 25-fold increase of the baseline level, which is about 2% for YRp4. The enhancement of knots was accompanied by a concomitant increase of the positive supercoiling [109], see Fig. 8.8.

The experiments, thus, gave a striking demonstration that, in the course of removing torsional stress, topoisomerases can transiently increase DNA knotting much above the homeostatic level, before eventually re-establishing the baseline entanglement.

Coarse-grained models based on strings and beads (used to model nucleosomes and linkers) were also used to rationalize the high level of transient knotting. The Monte Carlo simulations of the model YRp4 chromatin showed that the observed boost of knotting probability is compatible with a fivefold increase of compactification (i.e. decrease of gyration volume) of the chromosome [109], which is expectedly induced by the local accumulation of supercoiling during transcription.

The results open entirely new perspectives on the entanglement of eukaryotic genomes and prompt numerous questions. What amount of homeostatic knotting is actually present in much longer chromosomes than YRp4? How much can it increase during transcription and other enzymatic processing of DNA? Does chromatin entanglement play any role in structuring chromatin in vivo [109–111]? We expect that

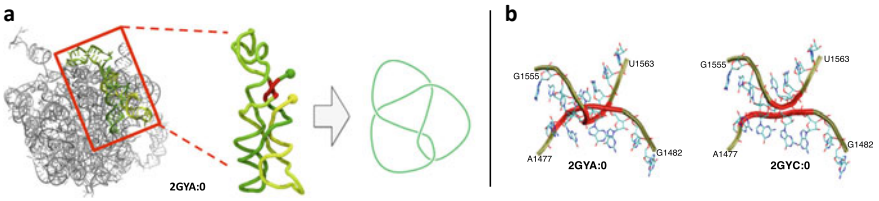

Fig. 8.9 **a** RNA conformation of PDB entry 2GYA:0 presents a physical knot, arising from the highlighted interlocking of two helices. **b** Comparison with a higher resolution homolog (PDB entry 2GYC:0), where the interlocking is not present, suggests the artefactual nature of the physical knot. Reproduced with permission from Ref. [5]

significant breakthroughs will be achieved in all these avenues with a synergistic effort of experiments, models, and simulations.

8.4 RNA (un)Knotting

We conclude this overview of knots in nucleic acids by extending considerations from DNA to RNA.

RNA filaments are flexible, their persistence length being about 1 nm, and their length can range from a few nucleotides to thousands of them, as for ribosomal units.

One might expect that RNA knotting properties are not different from those of other flexible biopolymers such as proteins. Regarding the latter, we recall that a few percent of protein PDB entries are physically knotted [112–115].

A first systematic survey of RNA knotting was carried out in Ref. [5] and gave a surprisingly negative outcome.

Out of the thousands of RNA entries present in the protein data bank at that time, only three putative knotted RNA structures were found, all solved by cryo-em. For two of them, there were available homolog structures solved by X-ray crystallography, which were unknotted. A detailed comparison of the cryo-em and X-ray versions revealed that the former featured interlocked RNA helices, which were instead well-separated and disentangled in the higher resolution X-ray counterpart; see, e.g. Fig. 8.9. The third knotted structure presented other issues, too, such as atypical bends of the RNA virtual backbone (P-trace). It was, thus, deemed that the crossings responsible for the putative knotted states of the three RNA entries were most likely artefactual [5].

The analysis, thus, gave the unexpected result that no knotted RNA entries existed among the thousands deposited in the PDB. The conclusion remained unchanged in a later survey on a larger dataset [6].

The result prompted several considerations and speculations too. The fact that knots have a much lower incidence in natural RNAs (where none has been found so far) compared to proteins suggests the possibility that the folding kinetics or

thermodynamics of naturally occurring RNAs has been co-opted by evolution to minimize the incidence of knots. For instance, secondary elements established during co-transcriptional folding of nascent RNAs may already decrease the knotting probability. Compared to an unstructured filament, it would be more difficult for a structured RNA to establish the loops and threadings conducive to knots. In addition, the RNA sequence itself may have evolved so that the native folded state can be established by accretion or modularly, which also would make RNA less prone to form knots [5].

It cannot be ruled out that genuinely knotted RNA structures can be found in the future with the growing size of the database. An indication that this is possible, or even likely, comes from the groundbreaking work of Seeman et al. [116] who, as early as 1996, succeeded at designing and synthesizing RNA strands of about 100 nucleotides that adopted knotted folds. As a matter of fact, there already exists circumstantial evidence pointing at the knotted state of certain natural RNAs [6]. However, a positive confirmation of their entanglement from direct structural determination is still pending.

While the quest for physically knotted RNAs is still open, it is appropriate to recall that RNAs are rich in other forms of entanglement or structural complexities termed pseudoknots. These structures are particularly common in viral RNAs where they serve different functional purposes such as causing ribosomal frameshifting [7–10] or resisting degradation by cellular defence mechanisms [11–17, 117]. Interestingly, in both cases, their functional role is to hinder RNA translocation through the lumen of enzymes, presenting, thus, qualitative analogies with translocating knotted chains.

It appears, thus, likely that further work on the properties of RNA secondary and tertiary elements can advance our understanding of the functional implications of entanglement in biomolecules.

8.5 Conclusions

Knots have been found in genomic DNA filaments of all organisms: from viruses to bacteria to eukaryotes. What we know today about the ubiquity of DNA entanglement in vivo and its quantification is the result of a long series of experimental breakthroughs, from trapping the transient DNA entanglement in robust topological states [23] to detecting the abundance of different knot types and their chirality too [26, 108] and to extending knot detection techniques to DNA strands of increasing lengths [118, 119].

The chase between new challenges and breakthroughs is not over yet, and theoretical models and numerical simulations play an essential part in it. Models with different levels of structural detail are indispensable to interpret experimental data and obtain the direct microscopic and dynamical insight that is often beyond the reach of experiments and are increasingly used to predict DNA entanglement properties. More than the complex biological contexts, such theoretical predictions are typically directed at nano-manipulation contexts, such as mechanical stretching and

translocation [77, 120], microfluidics [121–123], and confinement inside nanochannels, slits, and cavities [124–132]. These are all instances where the insight afforded by such approaches is advancing our understanding of the role of how the static and dynamics of polymers are affected by topology. This rapidly evolving field will undoubtedly expose many surprising and counter-intuitive results, most likely in the context of inter-molecular DNA entanglement.

Acknowledgements The material presented in this overview intersects the work of many colleagues and research groups that I had the pleasure to interact with during collaborations, visits, and exchanges and at conferences. For the topics touched here, I wish to recall, in particular, Lucia Coronel, Tetsuo Deguchi, Giovanni Dietler, Marco Di Stefano, Massimiliano Di Ventra, Alexander Grosberg, Davide Marenduzzo, Ken Millet, Henri Orland, Enzo Orlandini, Eric Rawdon, Joaquim Roca, Angelo Rosa, Andrzej Stasiak, Antonio Suma, De Witt Sumners, Erica Uehara, Yasuyuki Tezuka, and Luca Tubiana. I am indebted to many of them not only for having enriched me scientifically but also personally. I am also grateful to Prof. Yasuyuki Tezuka and Prof. Tetsuo Deguchi for the editing of this contribution.

References

1. D. Pawson, *Knot craft* (Adlard Coles Nautical, 2009)
2. L. Olavarrieta, P. Hernandez, D.B. Krimer, J.B. Schvartzman, J. Mol. Biol. **322**(1), 1 (2002)
3. R.W. Deibler, J.K. Mann, L.S. De Witt, L. Zechiedrich, BMC Mol. Biol. **8**(1), 44 (2007)
4. J. Portugal, A. Rodríguez-Campos, Nucleic Acids Res. **24**, 4890 (1996)
5. C. Micheletti, M. Di Stefano, H. Orland, Proc. Natl. Acad. Sci. **112**(7), 2052 (2015)
6. A.S. Burton, M. Di Stefano, N. Lehman, H. Orland, C. Micheletti, RNA Biol. **13**(2), 134 (2016)
7. D.P. Giedroc, P.V. Cornish, Virus Res. **139**(2), 193 (2009)
8. D.P. Giedroc, C.A. Theimer, P.L. Nixon, J. Mol. Biol. **298**(2), 167 (2000)
9. G. Chen, K.Y. Chang, M.Y. Chou, C. Bustamante, I. Tinoco, Proc. Natl. Acad. Sci. U.S.A. **106**(31), 12706 (2009)
10. S.Y. Le, B.A. Shapiro, J.H. Chen, R. Nussinov, J.V. Maizel, Gen. Anal.: Biomol. Eng. **8**(7), 191 (1991)
11. G.P. Pijlman, A. Funk, N. Kondratieva, J. Leung, S. Torres, L. Van der Aa, W.J. Liu, A.C. Palmenberg, P.Y. Shi, R.A. Hall, A.A. Khromykh, Cell Host Microbe **4**(6), 579 (2008)
12. E.G. Chapman, D.A. Costantino, J.L. Rabe, S.L. Moon, J. Wilusz, J.C. Nix, J.S. Kieft, Science **344**(6181), 307 (2014)
13. B.M. Akiyama, H.M. Laurence, A.R. Massey, D.A. Costantino, X. Xie, Y. Yang, P.Y. Shi, J.C. Nix, J.D. Beckham, J.S. Kieft, Science **354**(6316), 1148 (2016)
14. A. Slonchak, A.A. Khromykh, Antivir. Res. (2018)
15. A. MacFadden, Z. O'Donoghue, P.A. Silva, E.G. Chapman, R.C. Olsthoorn, M.G. Sterken, G.P. Pijlman, P.J. Bredenbeek, J.S. Kieft, Nat. Commun. **9**(1), 119 (2018)
16. W.C. Ng, R. Soto-Acosta, S.S. Bradrick, M.A. Garcia-Blanco, E.E. Ooi, Viruses **9**(6), 137 (2017)
17. A. Suma, L. Coronel, G. Bussi, C. Micheletti, Nat. Commun. **11**(1), 1 (2020)
18. D. Marenduzzo, C. Micheletti, E. Orlandini, J. Phys.: Condens. Matter **22**, 283102 (2010)
19. D. Meluzzi, D.E. Smith, G. Arya, Annu. Rev. Biophys. **39**, 349 (2010)
20. C. Micheletti, D. Marenduzzo, E. Orlandini, Phys. Rep. **504**, 1 (2011)
21. L. Dai, C.B. Renner, P.S. Doyle, Adv. Coll. Interface. Sci. **232**, 80 (2016)
22. V.V. Rybenkov, N.R. Cozzarelli, A.V. Vologodskii, Proc. Natl. Acad. Sci. U.S.A. **90**, 5307 (1993)

23. J.C.W.S.Y. Shaw, Science **260**, 533 (1993)
24. A. Stasiak, V. Katritch, J. Bednar, D. Michoud, J. Dubochet, Nature **384**(6605), 122 (1996)
25. J. Cebrián, M.J. Kadomatsu-Hermosa, A. Castán, V. Martínez, C. Parra, M.J. Fernández-Nestosa, C. Schaerer, M.L. Martínez-Robles, P. Hernández, D.B. Krimer, A. Stasiak, J.B. Schvartzman, Nucleic Acids Res. **43**(4), e24 (2015)
26. S. Trigueros, J. Arsuaga, M.E. Vazquez, D. Sumners, J. Roca, Nucleic Acids Res. **29**(13), E67 (2001)
27. C. Weber, A. Stasiak, P. De Los Rios, G. Dietler, Biophys. J. **90**(9), 3100 (2006)
28. D. Michieletto, D. Marenduzzo, E. Orlandini, Proc. Natl. Acad. Sci. **112**(40), E5471 (2015)
29. R.N. Irobalieva, J.M. Fogg, D.J. Catanese, T. Sutthibutpong, M. Chen, A.K. Barker, S.J. Ludtke, S.A. Harris, M.F. Schmid, W. Chiu et al., Nat. Commun. **6**(1), 1 (2015)
30. T. Deguchi, K. Tsurusaki, Lectures at Knots, vol. 96 (World Scientific, Singapore, 1997), pp. 95–122
31. E. Rawdon, A. Dobay, J.C. Kern, K.C. Millett, M. Piatek, P. Plunkett, A. Stasiak, Macromolecules **41**(12), 4444 (2008)
32. P. Virnau, Y. Kantor, M. Kardar, J. Am. Chem. Soc. **127**, 15102 (2005)
33. B. Marcone, E. Orlandini, A.L. Stella, F. Zonta, J. Phys. A: Math. Gen. **38**, L15 (2005)
34. L. Tubiana, A. Rosa, F. Fragiacomo, C. Micheletti, Macromolecules **46**, 3669 (2013)
35. M.K. Shimamura, T. Deguchi, Phys. Lett. A **274**, 184 (2000)
36. M.K. Shimamura, T. Deguchi, Phys. Rev. E **64**, 020801 (2001)
37. M.K. Shimamura, T. Deguchi, Phys. Rev. E **65**, 051802 (2002)
38. E. Orlandini, M.C. Tesi, S.G. Whittington, J. Phys. A: Math. Gen. **38**, L795 (2005)
39. P. Virnau, F.C. Rieger, D. Reith, Biochem. Soc. Trans. **41**, 528 (2013)
40. L. Coronel, E. Orlandini, C. Micheletti, Soft Matter **13**, 4260 (2017)
41. L. Lu, H. Zhu, Y. Lu, L. An, L. Dai, Macromolecules **53**(21), 9443 (2020)
42. L. Dai, P.S. Doyle, Macromolecules **51**(16), 6327 (2018)
43. E. Uehara, L. Coronel, C. Micheletti, T. Deguchi, React. Funct. Poly. **134**, 141 (2019)
44. J. Arsuaga, M. Vázquez, S. Trigueros, D.W. Sumners, J. Roca, Proc. Natl. Acad. Sci. U.S.A. **99**, 5373 (2002)
45. J. Arsuaga, M. Vázquez, P. McGuirk, S. Trigueros, D.W. Sumners, J. Roca, Proc. Natl. Acad. Sci. U.S.A. **102**, 9165 (2005)
46. S. Trigueros, J. Roca, BMC Biotechnol. **7**, 94 (2007)
47. R. Matthews, A.A. Louis, J.M. Yeomans, Phys. Rev. Lett. **102**, 088101 (2009)
48. D. Marenduzzo, C. Micheletti, E. Orlandini, D.W. Sumners, Proc. Natl. Acad. Sci. U.S.A. **110**(50), 20081 (2013)
49. D. Marenduzzo, E. Orlandini, A. Stasiak, D.W. Sumners, L. Tubiana, C. Micheletti, Proc. Natl. Acad Sci. U.S.A **106**(52), 22269 (2009)
50. C. Micheletti, D. Marenduzzo, E. Orlandini, D.W. Sumners, J. Chem. Phys. **124**, 064903 (2006)
51. F.W.W.J.P.J. Michels, J. Phys. A: Math. Gen. **22**, 2393 (1989)
52. J.P.J. Michels, F.W. Wiegel, Proc. R. Soc. Lond. **A403**, 269 (1986)
53. J. Arsuaga, R.K. Tan, M. Vazquez, D.W. Sumners, S.C. Harvey, Biophys. Chem. **101–102**, 475 (2002)
54. C. Micheletti, D. Marenduzzo, E. Orlandini, D.W. Sumners, Biophys. J . **95**, 3591 (2008)
55. V. Katritch, W.K. Olson, A. Vologodskii, J. Dubochet, A. Stasiak, Phys. Rev. E **61**, 5545 (2000)
56. Y. Kantor, M. Kardar, Phys. Rev. E **69**(2), 021806 (2004)
57. M. Muthukumar, Annu. Rev. Biophys. Biomol. Struct. **36**, 435 (2007)
58. P. Rowghanian, A.Y. Grosberg, Phys. Rev. E **86**(1), 011803 (2012)
59. T. Ikonen, A. Bhattacharya, T. Ala-Nissila, W. Sung, Phys. Rev. E **85**(5), 051803 (2012)
60. V.V. Palyulin, T. Ala-Nissila, R. Metzler, Soft Matter **10**(45), 9016 (2014)
61. J. Sarabadani, T. Ala-Nissila, J. Phys.: Condens. Matter **30**(27), 274002 (2018)
62. A. Meller, L. Nivon, D. Branton, Phys. Rev. Lett. **86**(15), 3435 (2001)
63. E.H. Trepagnier, A. Radenovic, D. Sivak, P. Geissler, J. Liphardt, Nano Lett. **7**(9), 2824 (2007)

64. J. Comer, V. Dimitrov, Q. Zhao, G. Timp, A. Aksimentiev, Biophys. J . **96**(2), 593 (2009)
65. R.Y. Henley, S. Carson, M. Wanunu, in *Progress in Molecular Biology and Translational Science*, vol. 139 (Elsevier, Amsterdam, 2016), pp. 73–99
66. M. Zwolak, M. Di Ventra, Rev. Mod. Phys. **80**(1), 141 (2008)
67. D. Branton, D.W. Deamer, A. Marziali, H. Bayley, S.A. Benner, T. Butler, M. Di Ventra, S. Garaj, A. Hibbs, X. Huang, S.B. Jovanovich, P.S. Krstic, S. Lindsay, X.S. Ling, C.H. Mastrangelo, A. Meller, J.S. Oliver, Y.V. Pershin, J.M. Ramsey, R. Riehn, G.V. Soni, V. Tabard-Cossa, M. Wanunu, M. Wiggin, J.A. Schloss, Nat. Biotechnol. **26**(10), 1146 (2008)
68. C. Cao, M.Y. Li, N. Cirauqui, Y.Q. Wang, M. Dal Peraro, H. Tian, Y.T. Long, Nat. Commun. **9**(1), 1 (2018)
69. P. Bandarkar, H. Yang, R.Y. Henley, M. Wanunu, P.C. Whitford, Biophys. J. (2020)
70. K. Luo, T. Ala-Nissila, S.C. Ying, A. Bhattacharya, Phys. Rev. Lett. **100**(5), 058101 (2008)
71. C. Plesa, D. Verschueren, S. Pud, J. van der Torre, J.W. Ruitenberg, M.J. Witteveen, M.P. Jonsson, A.Y. Grosberg, Y. Rabin, C. Dekker, Nat. Nanotechnol. **11**(12), 1093 (2016)
72. C.A. Merchant, K. Healy, M. Wanunu, V. Ray, N. Peterman, J. Bartel, M.D. Fischbein, K. Venta, Z. Luo, A.C. Johnson et al., Nano Lett. **10**(8), 2915 (2010)
73. T. Kubota, K. Lloyd, N. Sakashita, S. Minato, K. Ishida, T. Mitsui, Polymers **11**(1), 84 (2019)
74. J. Chuang, Y. Kantor, M. Kardar, Phys. Rev. E **65**(1), 011802 (2001)
75. A. Bhattacharya, W.H. Morrison, K. Luo, T. Ala-Nissila, S.C. Ying, A. Milchev, K. Binder, Eur. Phys. J. E **29**(4), 423 (2009)
76. M. Wanunu, W. Morrison, Y. Rabin, A.Y. Grosberg, A. Meller, Nat. Nanotechnol. **5**(2), 160 (2010)
77. A. Rosa, M. Di Ventra, C. Micheletti, Phys. Rev. Lett. **109**, 118301 (2012)
78. P. Szymczak, Eur. Phys. J. Spec. Topics **223**(9), 1805 (2014)
79. P. Szymczak, Sci. Rep. **6**(1), 1 (2016)
80. M. Wojciechowski, À. Gómez-Sicilia, M. Carrión-Vázquez, M. Cieplak, Mol. BioSyst. **12**(9), 2700 (2016)
81. Á. San Martín, P. Rodriguez-Aliaga, J.A. Molina, A. Martin, C. Bustamante, M. Baez, Proc. Natl. Acad. Sci. **114**, 9864 (2017)
82. M.K. Sriramoju, Y. Chen, Y.T.C. Lee, S.T.D. Hsu, Sci. Rep. **8**(1), 7076 (2018)
83. S.E. Jackson, Topol. Geometry Biopoly. **746**, 129 (2020)
84. K. Sishido, N. Komiyama, S. Ikawa, J. Mol. Biol. **195**(1), 215 (1987)
85. K. Shishido, S. Ishii, N. Komiyama, Nucleic Acids Res. **17**, 9749 (1989)
86. S.A. Wasserman, J.M. Dungan, N.R. Cozzarelli, Science **229**, 171 (1985)
87. J.M. Sogo, A. Stasiak, M.L. Martinez-Robles, D.B. Krimer, P. Hernandez, J.B. Schvartzman, J. Mol. Biol. **286**, 637 (1999)
88. V. López, M.L. Martínez-Robles, P. Hernández, D.B. Krimer, J.B. Schvartzman, Nucleic Acids Res. **40**, 3563 (2011)
89. J.C. Wang, Annu. Rev. Biochem. **65**, 635 (1996)
90. V. López, M.L. Martínez-Robles, P. Hernández, D.B. Krimer, J.B. Schvartzman, Nucleic Acids Res. **40**(8), 3563 (2012)
91. L.F. Liu, C.C. Liu, B.M. Alberts, Cell **19**, 697 (1980)
92. V. Rybenkov, C. Ullsperger, A.V. Vologodskii, N.R. Cozzarelli, Science **277**, 690 (1997)
93. R.W. Deibler, S. Rahmati, E.L. Zechiedrich, Genes Dev. **15**, 748 (2001)
94. D.E. Adams, E.M. Shekhtman, E.L. Zechiedrich, M.B. Schmid, N.R. Cozzarelli, Cell **71**, 277 (1992)
95. Z. Liu, R.W. Deibler, H.S. Chan, L. Zechiedrich, Nucleic Acids Res. **37**(3), 661 (2009)
96. T. Goto, J.C. Wang, J. Biol. Chem. **257**, 5866 (1982)
97. G.L. Randall, B.M. Pettitt, G.R. Buck, E.L. Zechiedrich, J. Phys.: Condens. Matter **18**, S173 (2006)
98. Z. Liu, J.K. Mann, E.L. Zechiedrich, H.S. Chan, J. Mol. Biol. **361**, 268 (2006)
99. Z. Liu, L. Zechiedrich, H.S. Chan, J. Mol. Biol. **400**(5), 963 (2010)
100. Z. Liu, H.S. Chan, J. Phys.: Condens. Matter **27**, 354103 (2015)
101. R. Ziraldo, A. Hanke, S.D. Levene, Nucleic Acids Res. **47**(1), 69 (2019)

102. G. Witz, A. Stasiak, Nucleic Acids Res. **38**, 2119 (2009)
103. G. Witz, G. Dietler, A. Stasiak, Proc. Natl. Acad. Sci. U.S.A. **108**, 3608 (2011)
104. D. Racko, F. Benedetti, J. Dorier, Y. Burnier, A. Stasiak, Nucleic Acids Res. **43**, 7229 (2015)
105. E.J. Rawdon, J. Dorier, D. Racko, K.C. Millett, A. Stasiak, Nucleic Acids Res. **44**, 4528 (2016)
106. L. Coronel, A. Suma, C. Micheletti, Nucleic Acids Res. **46**(15), 7533 (2018)
107. G.R. Buck, E.L. Zechiedrich, J. Mol. Biol. **340**(5), 933 (2004)
108. A. Valdés, J. Segura, S. Dyson, B. Martínez-García, J. Roca, Nucleic Acids Res. **46**(2), 650 (2018)
109. A. Valdés, L. Coronel, B. Martínez-García, J. Segura, S. Dyson, O. Díaz-Ingelmo, C. Micheletti, J. Roca, Nucleic Acids Res. **47**(13), 6946 (2019)
110. J.T. Siebert, A.N. Kivel, L.P. Atkinson, T.J. Stevens, E.D. Laue, P. Virnau, Polymers **9**(8), 317 (2017)
111. A. Rosa, M.D. Stefano, C. Micheletti, Front. Mol. Biosci. **6**, 127 (2019)
112. M.L. Mansfield, Nat. Struct. Biol. **1**(4), 213 (1994)
113. P. Virnau, A. Mallam, S. Jackson, J. Phys.: Condens. Matter **23**(3), 033101 (2011)
114. P. Dabrowski-Tumanski, J.I. Sulkowska, Polymers **9**(9), 454 (2017)
115. S.E. Jackson, A. Suma, C. Micheletti, Curr. Opin. Struct. Biol. **42**, 6 (2017)
116. H. Wang, R.J. Di Gate, N.C. Seeman, Proc. Natl. Acad. Sci. **93**(18), 9477 (1996)
117. M. Becchi, P. Chiarantoni, A. Suma, C. Micheletti, J. Phys. Chem. B **125**(4), 1098 (2021)
118. C. Plesa, D. Verschueren, S. Pud, J. van der Torre, J.W. Ruitenberg, M.J. Witteveen, M.P. Jonsson, A.Y. Grosberg, Y. Rabin, C. Dekker, Nat. Nanotechnol. **11**(12), 1093 (2016)
119. A. Suma, C. Micheletti, Proc. Natl. Acad. Sci. USA **114**(15), E2991 (2017)
120. A. Suma, A. Rosa, C. Micheletti, ACS Macro Lett. **4**(12), 1420 (2015)
121. C.B. Renner, P.S. Doyle, ACS Macro Lett. **3**, 963 (2014)
122. A.R. Klotz, V. Narsimhan, B.W. Soh, P.S. Doyle, Macromolecules **50**(10), 4074 (2017)
123. A.R. Klotz, B.W. Soh, P.S. Doyle, Phys. Rev. Lett. **120**, 188003 (2018)
124. R. Metzler, W. Reisner, R. Riehn, R. Austin, J.O. Tegenfeldt, I.M. Sokolov, Europhys. Lett. **76**(4), 696 (2006)
125. W. Mobius, E. Frey, U. Gerland, Nano Lett. pp. 4518–4522 (2008)
126. R. Matthews, A.A. Louis, J.M. Yeomans, Mol. Phys. **109**(7–10), 1289 (2011)
127. L. Tubiana, E. Orlandini, C. Micheletti, Phys. Rev. Lett. **107**, 188302 (2011)
128. C. Micheletti, E. Orlandini, Macromolecules **45**, 2113 (2012)
129. C. Micheletti, E. Orlandini, Soft Matter **8**, 10959 (2012)
130. P.K. Lin, C.C. Hsieh, Y.L. Chen, C.F. Chou, Macromolecules **45**, 2920 (2012)
131. E. Orlandini, C. Micheletti, J. Biol. Phys. **39**, 267 (2013)
132. S. Amin, A. Khorshid, L. Zeng, P. Zimny, W. Reisner, Nat. Commun. **9**(1), 1 (2018)